Journal of Inorganic Biochemistry 193 (2019) 112–123

Contents lists available at ScienceDirect

Journal of Inorganic Biochemistry

journal homepage: www.elsevier.com/locate/jinorgbio

Ruthenium(II) salicylate complexes inducing ROS-mediated apoptosis by targeting thioredoxin reductase

Jin-can Chen[a,b], Yao Zhang[c], Xin-ming Jie[a], Ji She[c], Guang-zhi Dongye[a], Yu Zhong[a], Yuan-yuan Deng[c], Jie Wang[c], Bo-yang Guo[d], Lan-mei Chen[c,*]

[a] Analysis Centre of Guangdong Medical University, Zhanjiang 524023, China
[b] Guangdong Key Laboratory for Research and Development of Nature Drugs, Guangdong Medical University, Zhanjiang 524023, China
[c] Dongguan Key Laboratory of Drug Design and Formulation Technology, School of Pharmacy, Guangdong Medical University, Dongguan 523808, China
[d] The First Clinical Medical College, Guangdong Medical University, Zhanjiang 524023, China

ARTICLE INFO

Keywords:
Ru (II) complexes
Salicylate
Apoptosis
Thioredoxin reductase
ROS

ABSTRACT

Thioredoxin reductase (TrxR), a major component of the thioredoxin system, makes a critical role in regulating cellular redox signaling and is found to be overexpressed in many human cancer cells. TrxR has become an attractive target for anticancer agents. In this work, three Ru(II) complexes with salicylate as ligand, [Ru(phen)$_2$(SA)] (phen = 1,10-phenanthroline, SA = salicylate, **1**), [Ru(dmb)$_2$(SA)] (dmb = 4,4′-dimethyl-2,2′-bipyridine, **2**) and [Ru(bpy)$_2$(SA)] (bpy = 2,2′-bipyridine, **3**), were synthesized and characterized. The anticancer effect exerted by them was evaluated. Complex **1** was found to exhibit obvious anticancer activity, in comparison with cisplatin, against cancer cell lines, while displaying low toxicity to the normal cell line BEAS-2B. The mechanism of complex **1** cancer cell growth suppress was investigated in A549 cells. Complex **1** exerted its anticancer through inducing apoptosis and triggering cell cycle arrest at the G0/G1 phase. Complex **1** can selectively inhibit TrxR activity and thus promote the generation and accumulation of reactive oxygen species (ROS), which subsequently trigger mitochondrial dysfunction and DNA damage, activate oxidative stress-sensitive mitogen activated protein kinase (MAPK), and suppress the protein kinase B (PKB or AKT) signal pathway, resulting in apoptosis in A549 cells.

1. Introduction

Aspirin (aspH, *o*-acetyl-salicylate) is one of the most widely used drugs worldwide, which can exert antipyretic, antiphlogistic and analgesic effect [1]. Salicylate (SA) (or *o*-hydroxybenzoic acid), a precursor of aspirin, also exhibits antiphlogistic activity and it has been applied as a drug [1]. Numerous epidemiological studies have demonstrated that long-term use of salicylate may reduce the risk of colon cancer by 40%–50%, and prevent suffering lung cancer, esophageal cancer and gastric cancer [2]. In addition, salicylate is a multifunctional ligand with two hard and strong alkaline donor centers promoting chelation or metal bridging of medium to large cations [3]. In recent time, it has reported that silver(I), copper(II) and organotin complexes with SA as ligand exhibit significant anticancer activity [2,4–7].

Recent decades, more and more reports believed that Ruthenium (Ru) complexes have emerged as the most outstanding candidate for cancer treatment [8]. So far three Ru complexes imidazolium [trans-RuCl$_4$(1H-imidazole)(DMSO-S)] (NAMI-A), indazolium [trans-RuCl$_4$(1H-indazole)$_2$] (KP1019) and sodium [trans-RuCl$_4$(1H-indazole)$_2$] (NKP-1339) have entered clinical trial [9–11]. We have synthesized a series of Ru complexes with β-carboline or imidazole as functional ligands, which exhibit significant antiproliferation effect on cancer cells [12,13]. Moreover, the recent studies by Chen et al. disclosed that the Ru polypyridyl complex [Ru(pip)$_3$]$^{2+}$ (pip = 2-phenylimidazo[4,5-f] [1,10]phenanthroline) induced reactive oxygen species (ROS)-mediated apoptosis in cancer cells by targeting thioredoxin reductase (TrxR) [14]. TrxR and thioredoxin (Trx), two main constituents of the thioredoxin system, play an important role in regulation of the redox balance and intracellular signaling pathways, and targeting these is a new strategy for cancer treatment [14–17].

TrxR maintains the redox balance of cells and regulates redox-mediated signal transduction by acting on its substrate molecule thioredoxin, which in turn controls the proliferation, differentiation and death of cells, as well as a series of biological processes [18]. More importantly, TrxR is highly expressed in various primary tumors, such as liver cancer and lung cancer [19]. Except for Trx, many endogenous

* Corresponding author.
E-mail address: lanmeichen@126.com (L.-m. Chen).

https://doi.org/10.1016/j.jinorgbio.2019.01.011
Received 7 September 2018; Received in revised form 19 January 2019; Accepted 20 January 2019
Available online 25 January 2019
0162-0134/

substrates have also been shown to be reduced by TrxR, such as lipoic acid, lipid peroxides and so on [20,21]. Besides, in contrast to those from bacteria, mammalian TrxRs are bulky selenium-containing proteins with a penultimate selenocysteine (Sec) in the C-terminal active site, which contributes to the broad substrate specificity of TrxR [22,23]. In addition, the Sec in the TrxR carbon terminal active site has a low p*K*a value, which makes the enzyme present high activity and react easily with electrophiles [24].

Currently, many studies have demonstrated that numerous anticancer agents could inhibit TrxR. For instance, cisplatin, one of the first therapeutically applied anticancer drugs, is found to act as an effective irreversible inhibitor of TrxR [25]. Auranofin, the first reported TrxR inhibitor, is ascertained that specifically acts on selenium groups on TrxR selenocysteine residues [26]. However, auranofin easily integrates with serum albumin in vivo and thus causes the rapid metabolism time of auranofin. A large amount of gold complexes have been synthesized and investigated for their inhibitory effect on TrxR. Ingo Ott et al. synthesized a series of gold complexes which exhibited significant inhibitory properties of TrxR through the gold atoms in the complexes covalently bonding to the carbon-terminal active site -Cys-SeCys- [15,27]. In 2007, Mura et al. initially reported that Ru complexes inhibited the activity of rat cytosolic TrxR [28]. Casini et al. found several Ru(II)-arene complexes could inhibit the activity of TrxR [29]. Therefore, the above evidences indicate that the Ru complexes could act as a potential kind of inhibitors of TrxR, and the inert Ru(II) complexes may exert their anticancer effect with the action of TrxR inhibition.

Encouraged by these findings, we synthesized three Ru(II) complexes with SA as main ligand, [Ru(phen)$_2$(SA)] (phen = 1,10-phenanthroline, **1**), [Ru(dmb)$_2$(SA)] (dmb = 4,4′-dimethyl-2,2′-bipyridine, **2**) and [Ru(bpy)$_2$(SA)] (bpy = 2,2′-bipyridine, **3**), and examined their anticancer activity. Their inhibitory effect on TrxR and anticancer mechanism were further investigated. Our findings show that, the synthetic Ru(II) complexes could induce ROS-mediated apoptosis through inhibiting TrxR activity. Mitochondrial dysfunction, DNA damage, activation of mitogen activated protein kinase (MAPK) and inhibition of protein kinase B (PKB or AKT) signaling pathway were also triggered in A549 cells exposed to complex **1**. These results indicate that Ru(II) salicylate complexes could be developed as TrxR-targeted agents that demonstrate application potentials for the cancer treatment.

2. Experimental section

2.1. Materials and physical measurements

All reagents and solvents were purchased commercially and used without further purification unless otherwise noted. Dimethylsulfoxide (DMSO), Phosphate buffered saline (PBS), propidium iodide (PI), 5,5′6,6′-tetrachloro-1,1′,3,3′-tetraethylimidacarbocyanine iodide (JC-1), 2,7-Dichlorodi-hydrofluorescein diacetate (DCFH-DA), Annexin V-fluorescein isothiocyanate (FITC) Apoptosis Detection Kit, QuantiPro™ BCA Assay Kit, ECL™ Start Western Blotting Detection Reagent were purchased from Sigma. Glutathione peroxidase (GSH-Px), glutathione reductase (GSH-Rs) activities assay kits and 3-(4,5-dimethylthiazole)-2,5-diphenyltetraazolium bromide (MTT) were purchased from Beyotime (Shanghai, China). Ru standard solution was purchased from Aladdin Chemistry Co. (Shanghai, China). Comet assay reagent kit was purchased from Trevigen (Gaithersburg, MD, USA). TrxR Activity Kit was purchased from Cayman Chemical. Roswell Park Memorial Institute (RPMI) 1640 and fetal bovine serum (FBS) were obtained from HyClone. Primary and secondary antibodies were purchased from Cell Signaling Technology Company. Protein bands were visualized using ChemiDoc™ XRS + Imaging System (Bio-Rad, USA). Microanalyses (C, H, and N) were obtained with a Perkin–Elmer 240Q elemental analyzer. Mass analysis was performed on a 6430A triple – quadrupole mass spectrometer (Agilent Technologies, USA) using CH_3CN as mobile phase. ^{1}H NMR spectra was recorded on a Bruker AVANCE 400 spectrometer (400 MHz) at room temperature. UV–visible (UV–Vis) spectra were measured on Perkin–Elmer Lambda-850 spectrophotometer at 25 °C. Flow cytometry was performed by EPICS XL-MCL (BECKMAN COULTER, USA). Fluorescence microscope observation was performed by Ti-E (Nikon, Japan). Microplate was read by Tecan Infinite M200 pro.

2.2. Synthesis and characteristics

2.2.1. Synthesis of [Ru(phen)$_2$(SA)] (1)

A mixture of cis-[Ru(phen)$_2$Cl$_2$] (0.057 g, 0.1 mmol), *o*-hydroxybenzoic acid (0.0205 g, 0.15 mmol) and sodium hydroxide (0.012 g, 0.3 mmol) were dissolved in ethanol and water mixed solution (1:1), and then the mixture was refluxed under nitrogen for 11 h to appear a clear red solution. And then the solution was cooled to room temperature, concentrated by rotary evaporator. Finally, the precipitate was dried in vaccum and purified by chromatography over alumina (200 mesh) using ethanol/water - (1:1, v/v) as an eluent. Yield: 81.8%. ^{1}H NMR (400 MHz, DMSO-d_6): δ 9.43 (dd, ^3J = 5.2, ^4J = 1.2 Hz, 1H), 9.35 (dd, ^3J = 5.2, ^4J = 1.3 Hz, 1H), 8.66 (dd, ^3J = 8.1, ^4J = 1.3 Hz, 2H), 8.35–8.24 (m, 4H), 8.20 (m, 2H), 8.09 (m, 2H), 7.83 (dd, ^3J = 5.5, ^4J = 1.2 Hz, 1H), 7.87 (dd, ^3J = 5.4, ^4J = 1.2 Hz, 1H), 7.70 (dd, ^3J = 7.9, ^4J = 2.0 Hz, 1H), 7.40 (td, ^3J = 7.9, 5.3 Hz, 2H), 6.73 (ddd, ^3J = 8.6, 6.8, ^4J = 2.1 Hz, 1H), 6.28 (dd, ^3J = 8.5, ^4J = 1.3 Hz, 1H), 6.15 (ddd, ^3J = 7.9, 6.7, ^4J = 1.3 Hz, 1H). Electrospary ionization mass spectrometry (ESI-MS) (MeCN): m/z = 598.99 ([M + H]$^+$). UV–Vis (λ/nm, ε/M^{-1}·cm^{-1}) (CH_3CH_2OH): 266(41900), 512(6500). Anal. calc. for $C_{31}H_{20}N_4O_3Ru$: C, 62.31; H, 3.37; N, 9.38; found: C, 62.29; H, 3.36; N, 9.58.

2.2.2. Synthesis of [Ru(dmb)$_2$(SA)] (2)

Complex **2** was prepared by a similar procedure of **1**. ^{1}H NMR (400 MHz, $CDCl_3$): δ 8.80 (m, 1H), 8.71 (m, 1H), 8.63 (m, 1H), 8.48 (m, 1H), 8.26 (m, 1H), 8.13 (m, 1H), 7.97–7.89 (m, 4H), 7.82 (m, 1H), 7.69 (m, 1H), 7.60 (m, 1H), 7.42 (m, 1H), 7.27 (m, 1H), 6.74 (m, 1H), 3.43–3.25 (s, 6H), 2.55–2.47 (s, 6H). ESI-MS (MeCN): m/z = 607.06 ([M + H]$^+$). UV–Vis (λ/nm, ε/M^{-1}·cm^{-1}) (CH_3CH_2OH): 294(17950), 360(5375), 534(3775). Anal. calc. for $C_{31}H_{28}N_4O_3Ru$: C, 61.48; H, 4.66; N, 9.25; found: C, 61.28; H, 4.66; N, 9.27.

2.2.3. Synthesis of [Ru(bpy)$_2$(SA)] (3)

Complex **3** was prepared by a similar procedure of **1**. ^{1}H NMR (400 MHz, DMSO-d_6): δ 9.01 (d, ^3J = 5.6, ^4J = 1.2 Hz, 1H), 8.97 (d, ^{3KKK}J = 5.6, ^4J = 1.2 Hz, 1H), 8.70 (d, ^3J = 8.1 Hz, 2H), 8.58 (d, ^3J = 8.1 Hz, 2H), 8.09–7.95 (m, 2H), 7.79–7.70 (m, 2H), 7.70–7.62 (m, 3H), 7.56 (t, ^3J = 6.0, ^4J = 1.1 Hz, 2H), 7.15 (m, 2H), 6.73 (ddd, ^3J = 8.6, 6.7, ^4J = 2.1 Hz, 1H), 6.30 (dd, ^3J = 8.4, ^4J = 1.3 Hz, 1H), 6.13 (ddd, ^3J = 8.0, 6.7, ^4J = 1.3 Hz, 1H). ESI-MS (MeCN): m/z = 550.99 ([M + H]C$^+$). UV–Vis (λ/nm, ε/M^{-1}·cm^{-1}) (CH_3CH_2OH): 295(58600), 367(11150), 526(9050). Anal. calc. for $C_{27}H_{20}N_4O_3Ru$: C, 59.01; H, 3.67; N, 10.20; found: C, 58.95; H, 3.68; N, 10.20.

2.3. Cell lines and culture conditions

Human cancer cell lines studied in this work were all obtained from American Type Culture Collection (ATCC, Manassas, VA). All cell lines were maintained in RPMI 1640 culture media supplemented with 10% FBS and incubated at 37 °C in a 5% CO_2 incubator unless otherwise noted.

2.4. Cytotoxicity assay in vitro

Cells were seeded in 96-well plates and incubated for 12 h. Various concentrations of complexes tested were added to the wells. Cisplatin was used as positive control. After incubation for 48 h, stock MTT dye solution was added to each well and incubated for 4 h. Then DMSO

(150 μL/well) was added to solubilize the MTT formazan forming in the living cells. The absorbance of the solution was measured by a microplate spectrophotometer at a wavelength of 570 nm, and the reference wavelength was set at 630 nm. The IC_{50} values were obtained from the analysis of absorbance data.

2.5. Cellular uptake and localization

The cells were cultured in 60 mm tissue culture dishes for 12 h before treatment with 32 μM complexes for different times. After treatment, the cells were collected. For localization, the nuclear, mitochondrial and cytoplasmic fractions of the A549 cells were extracted by using Cell Mitochondria Isolation Kit. The pellets were digested with 3 mL concentrated nitric acid and 1 mL perhydrol for 24 h, and then diluted to 5 mL with ultrapure water. Finally, the solutions were used for Inductively Coupled Plasma Mass Spectrometry (ICP-MS) to determine the amount of Ru complexes uptaken by human lung carcinoma A549 cells.

2.6. Distribution coefficients

The distribution coefficient of each complex, which was presented as $\log P_{o/w}$ values, was detected by the "shake-flask" method as previously described. $\text{Log}P_{o/w}$ represents the logarithmic ratio of Ru(II) dose in n-octanol to that in aqueous phase [12].

2.7. Binding studies between complex *1* and TrxR model peptide

Complex **1** (0.08 mM in C_2H_5OH, solution A) and GCUG (0.4 mM in H_2O containing 5 mM NH_4HCO_3, solution B) were freshly prepared. Then 500 μL of solution A + 500 μL of H_2O (containing 5 mM NH_4HCO_3), or 500 μL of solution B + 500 μL of C_2H_5OH, or 500 μL of solution A + 500 μL of solution B were measured by ESI-MS at 0 h, 6 h and 12 h.

2.8. Determination of TrxR, glutathione peroxidase (GSH-Px) and glutathione reductase (GSH-Rs) activities in A549 cells

The cellular proteins of A549 cells treated with complexes were extracted and the BCA assay conducted to determine the concentration. The inhibition on TrxR activities induced by complexes were examined by Cayman's thioredoxin reductase assay kit follow the manufacturer's instructions, while the inhibition on activities of GSH-Px and GSH-Rs induced by complexes were determined by the specific kits purchased from Beyotime Institute of Biotechnology.

2.9. Cell cycle arrest analysis

Cell cycle distribution and apoptosis were analyzed by flow cytometry as described previously [13]. A549 cells were incubated with different doses of Ru complexes for 24 h, then collected and fixed in 75% ethanol at −20 °C overnight. The pellets were centrifuged and washed with PBS twice, subsequently stained with PI in the presence of RNAase A (100 μM) for 30 min at 37 °C in the dark. Then the samples were analyzed using a flow cytometer.

2.10. Apoptosis assay by Hoechst 33342 staining

A549 cells incubated in six-well plates were exposed to complexes for 24 h. And then, cells were stained with Hoechst 33342 (5 μg/mL) for 10 min and washed twice with PBS. Cell images were captured by an inverted fluorescence microscope.

2.11. Apoptosis assay by annexin V/PI double staining

The detection was performed by the AnnexinV-FITC Apoptosis Detection Kit as previously described [12]. After treatment with different concentration of the test complexes, A549 cells were harvested, washed twice in PBS, and then suspended in 500 μL binding buffer. The suspension was stained with AnnexinV-FITC and PI at room temperature for 15 min in the dark, and immediately determined by flow cytometry.

2.12. ROS assay

ROS level was detected after A549 cells had been stained with DCFH-DA as previously described [13]. After being cultured for 12 h, A549 cells were treated with various concentrations of complexes. For flow cytometry analysis or microplate analysis, the cells were collected and then incubated for 20 min with 10 mM DCFH-DA in culture medium at 37 °C in the dark. Cells were washed twice and resuspended in PBS, and then analyzed by a flow cytometer or a microplate analyzer. For microscopic observation, cells were incubated for 20 min in complete medium containing 10 mM DCFH-DA and washed twice with PBS, and then photographed by an inverted fluorescence microscope.

2.13. Mitochondrial membrane potential (MMP) measurement

Evaluation of mitochondrial depolarization was performed by measuring changes in the MMP as previously described [13]. A549 cells were incubated in medium containing compounds tested for 12 h. For flow cytometry analysis, the cells were collected and incubated in 500 μL PBS containing 10 μg/mL JC-1 for 30 min at 37 °C in the dark. The cells were analyzed by flow cytometer immediately. For microscope observation, the cells were incubated in complete medium containing 10 μg/mL JC-1 for 30 min and washed with PBS twice, and then analyzed by an inverted fluorescence microscope.

2.14. Comet assay

DNA damage, which was visualized by the comet tails, was examined by single-cell gel electrophoresis as previously described [30]. Single-cell gel electrophoresis was performed using the Comet assay reagent kit purchased from Trevigen according to the manufacturer's instructions. DNA was stained with SYBR Green I (Trevigen) and photographed by an inverted fluorescence microscope.

2.15. Western blotting analysis

The western blot assay was performed as previously described [31].

3. Results and discussion

3.1. Synthesis and characterization

Three Ru(II) complexes with SA as ligand, whose structures were shown in Fig. 1, were obtained through cis-$[Ru(N\text{-}N)_2Cl_2]$ (N-N = phen, dmb, bpy) reacting with SA in the presence of sodium hydroxide. Then the rough production was purified by the column chromatography to acquire desired Ru complexes. Three Ru(II) complexes were confirmed by elemental analysis, ESI-MS and ^1H NMR (Figs. S1–S11). All of the anticipated signals were presented in the ESI-MS spectra of the Ru(II) complexes. And the molecular weights detected were consistent with anticipated values.

The ^1H-^1H COSY of complexes **1** and **3** were provided in Figs. S4 and S11. The δ(H) were assigned by comparing with those of similar complexes [32]. Due to the asymmetry of the complexes, the δ values of two hydrogen atoms at the same position on the two ancillary ligands (bpy or phen) are slightly different in the NMR spectrum. And we think the δ(H) of the pyridine ring next to the salicylate ligand in the ancillary ligand is higher than that of the other pyridine ring. Since the bond of O = C–O– exhibits stronger electronegativity than the bond of –C–O–,

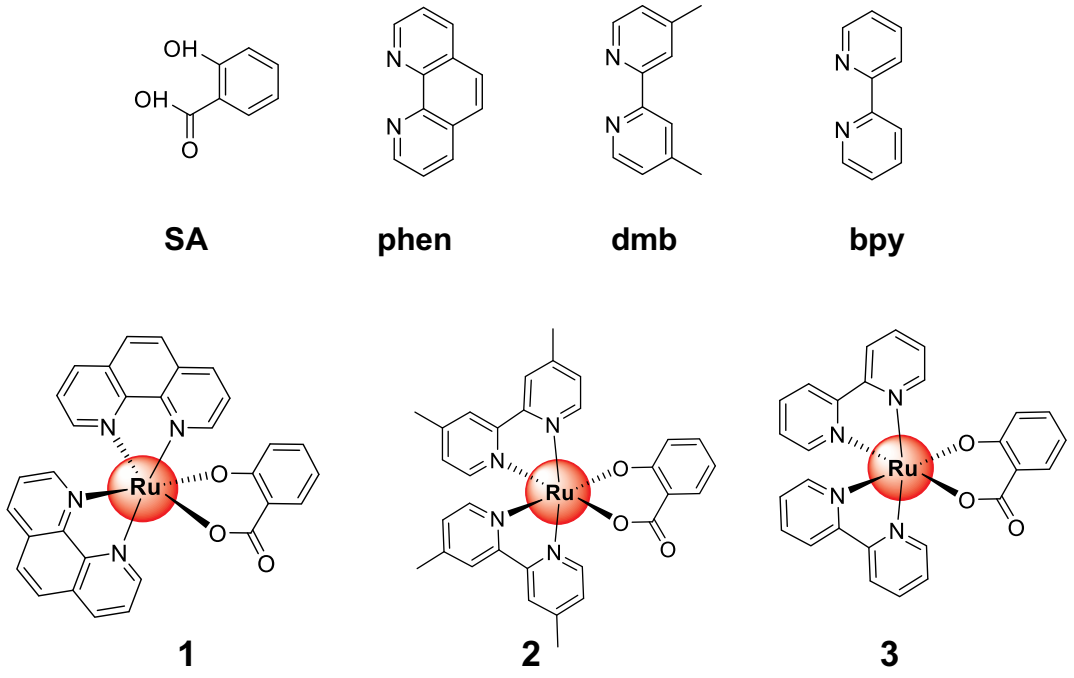

Fig. 1. The structures of Ru(II) complexes **1**, **2**, **3** and the ligands of SA, phen, dmb and bpy.

we speculate that the δ(H) of the ancillary ligand (bpy or phen) closing to the bond of O = C–O– is higher than that of the ancillary ligand closing to the bond of –C–O–. Taking complex **1** as an example, the peaks of H2 and H2′ or H9 and H9′ are completely apart. And the H2′ and H9′ are close to the bond of O = C–O–, whose shifts are higher than the shifts of H2 and H9 next to the bond of –C–O–. The shifts of H3′, H5′, H6′ and H7′ are greater than that of H3, H5, H6 and H7 respectively. However, the peaks of H3′, H5′, H6′ and H7′ partially overlap with the peaks of H3, H5, H6 and H7 respectively, which makes them exhibit multiple peaks, and the coupling constants cannot be determined. H4 and H4′ should have presented dd peak. But the peak of H4 partially overlaps with the peak of H4′, causing them exhibit triple type peaks.

3.2. Cytotoxicity assay in vitro

The cytotoxicities of the ligand SA, three Ru(II) synthetic precursors *cis*-[Ru(phen)$_2$Cl$_2$], *cis*-[Ru(dmb)$_2$Cl$_2$], *cis*-[Ru(bpy)$_2$Cl$_2$] and corresponding Ru(II) salicylate complexes against A549 (lung adenocarcinoma cell), HeLa (cervical cancer), MCF-7 (breast cancer), HepG2 (hepatocellular carcinoma) and normal human cell line BEAS-2B (immortalized human bronchial epithelial cells) were determined by MTT assay. In the meantime, the toxicity of cisplatin was tested as control. As shown in Table 1, prominent differences that beyond expectations are observed. Ru(II) salicylate complexes exhibiting much higher antiproliferation activities than the ligand salicylate and three Ru(II) synthetic precursors, which exhibit little toxicity toward all the cell lines tested (IC_{50} > 200 μM). Meanwhile, Ru(II) salicylate complexes exhibited a broad spectrum of inhibition on human cancer cells, with IC_{50} values ranging from 17.7 ± 1.3 to 48.2 ± 3.5 μM, which were comparable with those of cisplatin. Notably, synthetic Ru(II) salicylate complexes, especially complex **1**, presents much higher toxicity to cancer cell lines than to normal cell lines, while cisplatin exhibits almost equal toxicity between cancer cell lines and normal cell lines. From Table 1, we can also get that, the safer indexes of three Ru(II) salicylate complexes were calculated at 3.50, 1.78 and 1.58, respectively, which are much higher than that of cisplatin (0.79). The above results imply that three Ru(II) salicylate complexes presents high selectivity between cancer cells and normal cells.

The results distinctly demonstrate that the coordination of the SA ligand to polypyridyl-Ru(II) centers is a significant strategy for obtaining more cytotoxic complexes. More interestingly, the IC_{50} values of complex **1** is more potent than those of complexes **2** and **3** against all the test cancer cell lines screened under identical condition at 48 h treatment, especially A549 cells. Hence, we chose A549 cell as a cell model for further investigation of the anticancer mechanisms of complex **1**.

Table 1
Cytotoxic effects of Ru(II) complexes on human cancer and normal cell lines[a].

Complexes	IC_{50} (μM)					
	A549	Hela	MCF-7	HepG2	BEAS-2B	SI
Ru(phen)$_2$Cl$_2$	> 200	> 200	> 200	165.8 ± 5.8	–	–
Ru(dmb)$_2$Cl$_2$	> 200	> 161.0 ± 6.3	> 200	168.3 ± 6.2	–	–
Ru(bpy)$_2$Cl$_2$	> 200	> 200	> 200	181.0 ± 6.3	–	–
SA	> 200	> 200	> 200	> 200	–	–
1	17.7 ± 1.3	26.9 ± 1.9	34.7 ± 2.8	26.9 ± 2.7	62.5 ± 2.4	3.50
2	28.1 ± 1.2	29.4 ± 2.1	38.5 ± 2.7	31.6 ± 2.4	50.1 ± 2.7	1.78
3	40.5 ± 2.7	48.2 ± 3.5	40.2 ± 3.6	43.5 ± 2.5	64.3 ± 3.4	1.58
Cisplatin	27.2 ± 1.4	18.2 ± 1.2	16.2 ± 1.9	30.1 ± 2.0	21.4 ± 1.5	0.79

[a] Cells were treated with various concentrations of Ru(II) complexes for 48 h. Cells viability was determined by MTT assay to acquire IC_{50} values. Each value represents the mean ± SD of three independent experiments. SI (safer index) = IC_{50} (BEAS-2B)/IC_{50} (A549).

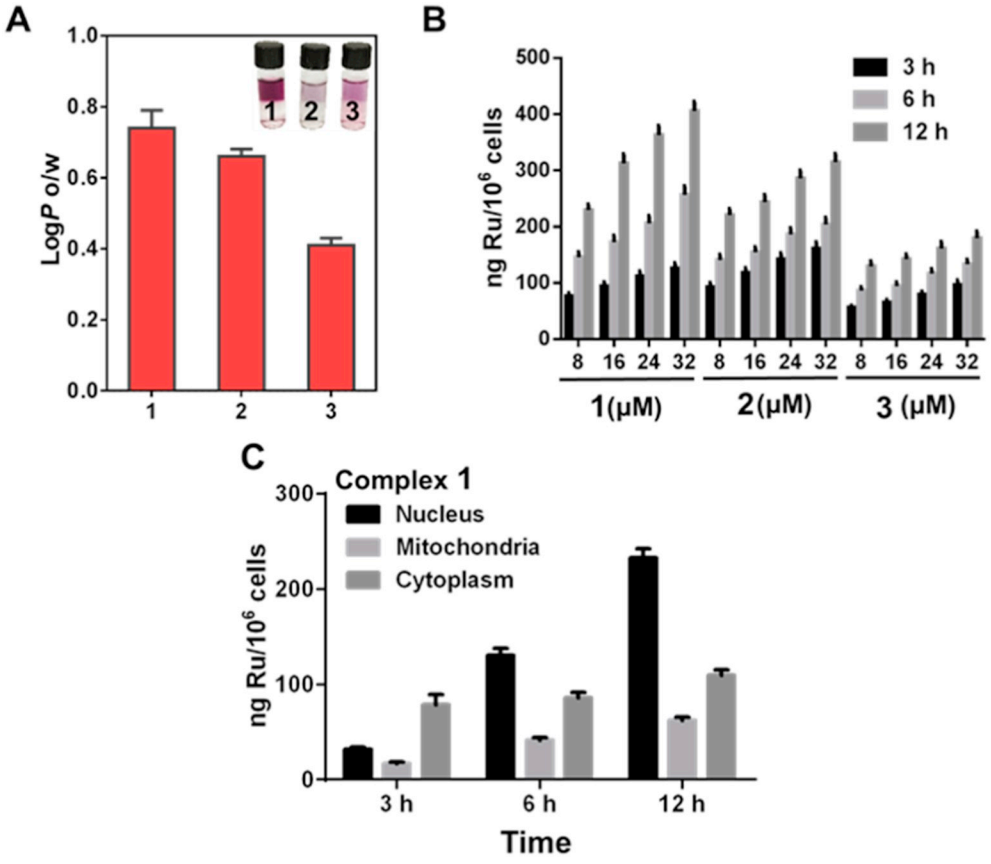

Fig. 2. (A) The log$P_{o/w}$ values of Ru(II) complexes **1**, **2**, **3**. (B) Cellular Ru concentrations determined in A549 cells after 3, 6 and 12 h incubated with complexes **1**, **2** and **3** at 8, 16, 24 and 32 μM, respectively. (C) Subcellular distribution of complex **1** in A549 cells after incubated with 32 μM of complex **1** for different times.

3.3. The cellular uptake and subcellular distribution of Ru(II) complexes

As everyone knows, the lipophilicity of an anticancer agent plays an important role in its cytotoxicity. Prior studies for ruthenium [33–35] and platinum based compounds [36,37] demonstrated that increasing lipophilicities enhanced the cellular uptake and subsequently resulted in high cytotoxic activities. The lipophilicity can be quantitatively estimated by log$P_{o/w}$ values, where P is the partition coefficient between octanol and water. Thus, the log$P_{o/w}$ of the synthesized Ru(II) salicylate complexes was examined by "shake-flask" method using ICP-MS. As seen in Fig. 2A, all the three Ru(II) complexes exhibit positive log$P_{o/w}$ values, implying that they are inherently lipophilic. Moreover, the log$P_{o/w}$ values of complexes **1–3** are 0.74 ± 0.05, 0.66 ± 0.02 and 0.41 ± 0.01 respectively, indicating complex **1** displays highest log$P_{o/w}$ value. Such result is in agreement with the previous report, that is, there is a positive correlation between hydrophobicity and cytotoxic activity for many transition metal-based anticancer agents [33,38–40].

The cellular uptake properties are regarded as one of the important factors that influence the cytotoxicity of transition metal-based drugs [41–43]. To study the possible relationship between the amount of cellular uptake and cytotoxic activities of synthetic Ru(II) salicylate complexes, ICP-MS was applied to quantitatively determine the Ru level inside the A549 cells. As displayed in Fig. 2B, the cellular uptakes of Ru (II) complexes exhibit significant dose- and time-dependent manners. Moreover, among all of Ru(II) complexes in all of the test time and drug concentrations, complex **1** presents the highest cellular uptake, which is positively correlated to their cytotoxicity and lipophilicity.

In addition, we employed ICP-MS to examine the subcellular distribution of complex **1** in A549 cells. As shown in Fig. 2C, we found that complex **1** mainly localized in the nuclei and merely a handful of complex **1** accumulated in cytoplasm and mitochondria, which indicated the localization of complex **1** in cell nucleus. Treating with complex **1** at a dose of 32 μM for 12 h, nearly 70% of this complex within the A549 cells accumulated in the nuclei. These results indicate that complex **1** targets the nuclei, which likes cyclometalated Ru(II) complexes, $[Ru(N\text{-}N)_2(1\text{-}Ph\text{-}\beta C)](PF_6)$ (N-N = bpy and dmb, 1-Ph-βC = 1-phenyl-9*H*-pyrido[3,4-*b*]indole) and $[Ru(bpy)(phpy)(dppz)]^+$ (phpy = 2-phenylpyridine, dppz = dipyrido[3,2-a:2′,3′-c]-phenazine) [12,44].

3.4. Ru(II) complexes inhibit cancer cells proliferation by targeting TrxR

Since its vital influence on regulating cellular redox balance and signaling pathways, TrxR is becoming an attractive target for anticancer drug development [45]. Moreover, metal-based complexes were reported to induce cell death through inhibiting TrxR activity, consequently suppressing the cancer cell progression [46]. Recently, Chen et.al found that Ru(II) polypyridyl complexes exhibited anticancer activities against human melanoma cells A375 through inhibiting TrxR activity and increasing ROS generation [14]. Encouraged by these results, we determined to investigate whether our synthetic Ru(II) complexes could act as TrxR inhibitors. According to previous studies [47], we adopt the C-terminal GCUG motif (Gly-Cys-Sec-Gly) to check for the binding of the complexes to TrxR's active site. The incubation of complex **1** with GCUG (1:5) (both have a linear response of MS intensity versus concentrations 0.003125–0.05 mM, 0.025–0.4 mM, respectively, Fig. S12) in 5 mM NH_4HCO_3 with 50% C_2H_5OH (v/v) for 6 h and 12 h results in significantly decrease in the MS intensities of complex **1** and GCUG (Fig. 3A). In the meanwhile, we hardly observed any changes in MS intensities of complex **1** and GCUG after incubating complex **1** or GCUG alone for 6 h and 12 h (Figs. S13, S14). We further examined the changes in MS intensity of mixtures of complex **1** over time. As

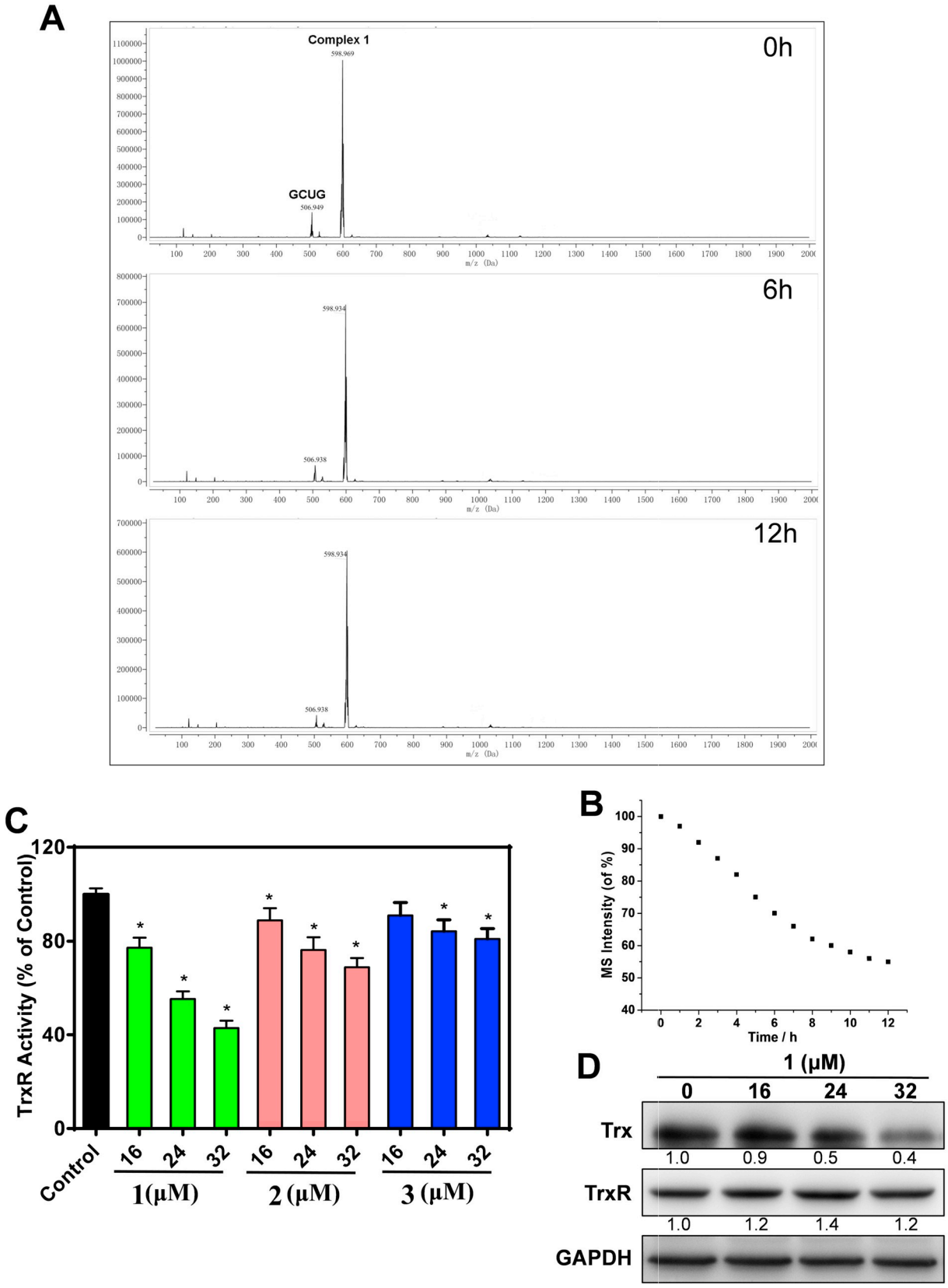

Fig. 3. (A) Interaction between complex **1** and TrxR. The ESI-MS analysis of mixture of complex **1** and GCUG in 0 h (up), 6 h (middle) and 12 h (down). Ru (II) complexes suppress the cancer cell progression by inhibiting TrxR. (B) The MS intensity of complex **1** after adding GCUG determined by ESI-MS. (C) TrxR activities in A549 cells after treatment with Ru(II) complexes. Significant difference between treatment and control groups is indicated at $P < 0.05$(*) levels. (D) Western blot analysis of the expression levels of TrxR and Trx in A549 cells after treatment with various concentrations of complex **1**. GAPDH was used as a loading control.

presented in Fig. 3B, the MS intensity of complex **1** decreases significantly with timescale. These results demonstrate that complex **1** may interact with GCUG. In general, inhibiting TrxR activity requires for a soft ligand-exchange reaction with thiols [48]. Thus, the stability of complex **1** toward bovine serum albumin (BSA) and glutathione (GSH) was subsequently determined. We employed UV–vis spectra to examine the interaction between complex **1** and BSA (or GSH) according to previous studies [49]. As shown in Fig. S15, after 12 h of incubation with excessive GSH or BSA, little change was observed in the characteristic absorption of complex **1**, which forcefully confirmed that complex **1** was inactive toward blood thiols. Moreover, the results of ESI-MS ascertained the above findings. As exhibited in Fig. S16, there was no significant change observed in MS spectra after mixing complex **1** with GSH for 12 h, demonstrating that complex **1** did not react with GSH. ICP-MS analysis also suggested that the synthetic Ru(II) complexes did not bind to BSA, especially complex **1** (Fig. S17). All of these findings demonstrate that complex **1** could selectively interact with TrxR.

Inspired by above results, we further investigated the inhibitory effect of complex **1** on TrxR activities of A549 cancer cells. From Fig. 3C, we can see that, the synthetic Ru(II) complexes induced TrxR inhibition in a dose-dependent manner. Furthermore, under the same concentration, complex **1** exhibits the most effective inhibition on TrxR activity, which is positively correlated with their cytotoxicity against A549 cell lines. The result of western blotting analysis presents no obvious change in the expression level of TrxR but apparent decline in the expression of Trx after treating A549 cells with complex **1** for 24 h (Fig. 3D), indicating complex **1** inhibits the activity of TrxR primarily by targeting active site of TrxR, rather than influencing the expression of TrxR. As the structural and functional similarity with TrxR, GSH-Rs was employed as a reference for detecting the enzyme inhibition specificity [15]. So we examined the activity of GSH-Rs in A549 cells treated with complex **1**. The intracellular activity of GSH-Rs is not distinctly affected by complex **1** at the concentrations of 16 μM, 24 μM and 32 μM, respectively (Fig. S18A). At the same time, we examined the activity of GSH-Px which is also one of the main intracellular selenoenzymes that could keep the cell redox balance [50]. As manifested in Fig. S18B, the intracellular activity of GSH-Px presents little difference after A549 cells exposed to complex **1**.

Therefore, the above acquired results imply that the synthetic Ru(II) complexes are potent to act as TrxR inhibitors. Taken together, we can infer that complex **1** selectively inhibit the activity of TrxR.

3.5. Ru(II) complexes induce cell cycle arrest and A549 cell apoptosis

Inducing apoptosis and cell cycle arrest are two main factors contributing to the inhibition of cell growth [51]. Firstly, the Hoechst 33342 staining technique for fluorescence microscope was initially carried out to determine apoptosis in A549 cells induced by synthetic Ru(II) complexes. From Fig. 4A, the complex **1**-treated cells with apoptotic features such as nuclear fragmentation, chromatin condensation and plasma membrane blebbing were notably observed. Less pronounced apoptotic features also can be seen in cells treated with complexes **2** and **3**. Complexes **1**–**3** can induce apoptosis in A549 cells. This promotes us to determine the percentage of apoptotic cells after annexinV-FITC/PI staining by using flow cytometry. A549 cells were treated with complex **1** ranging from 16 μM to 32 μM for 24 h. As shown in Fig. 4B, the percentages of apoptotic cells are increased from 3.24% (control) to 11.43%, 20.67% and 32.31% respectively, demonstrating that complex **1** induces A549 cells apoptosis in a dose-dependent manner. From Fig. S19, complexes **2** and **3** exhibited lower apoptotic effect than that of complex **1** as reflected by the percentage of apoptotic cells, which is in accordance with their anticancer activities. Additionally, western blotting was performed to ascertain the apoptosis in A549 cells induced by complex **1**. Caspases have been confirmed by a large amount of evidence to play a critical role for initiation and performance of apoptosis [52–54]. Based on the cleavage of caspases, apoptotic pathways can be divided into the extrinsic and intrinsic pathways [55]. After A549 cells were treated with complex **1**, the expression level of total caspase-3 decreases and the expression levels of cleaved-poly(ADP-ribose) polymerase (PARP), cleaved caspase-3 and cleaved caspase-9 increase obviously, but the expression of cleaved caspase-8 is not detected (Fig. 4D). This result indicates that only intrinsic apoptotic pathways contribute for the apoptosis induced by complex **1**.

Secondly, flow cytometry analysis was performed to detect the effect of complex **1** on cell cycle distribution. Fig. 4C showed that after complex **1** treatment, the percentage of cells at G0/G1 phase increased from 55.64% to 76.73%, demonstrating that the inhibition on cell growth induced by complex **1** occurs in G0/G1 phase. Besides, as seen in Fig. S20, the percentage of cells at G0/G1 phase increased from 58.36% to 72.85% after complex **2** treatment, which indicating complex **2** also inhibits cell growth at G0/G1 phase. The molecular basis by which complex **1** inhibit the G0/G1 transition in cancer cells was subsequently investigated. We treated A549 cells with complex **1** and then analyzed the expression of proteins involved in cell cycle regulation. As seen in Fig. 4E, complex **1** inhibits the expression of Cyclin D1/D3 and reduces the expression of Cyclin-dependent kinase 4/6 (CDK4 and CDK6), while promoting the expression of p27, p21 and p18. Cyclin D (along with CDK4 and CDK6) plays vital role in the cell progression through the G1 phase of the cell cycle [56]. The Cip/Kip family proteins p27, p21 and p18 are well-known CDK inhibitors and up-regulation the expression levels of those proteins can block G1-S transition [57]. These results indicate that complex **1** induces A549 cells apoptosis through intrinsic apoptotic pathway and triggers G0/G1 phase arrest to contribute for inhibition of cell growth.

3.6. Important roles of ROS in cell apoptosis induced by complex 1

ROS can affect MMP and then cause a chain of mitochondria-associated events, such as apoptosis [58]. However, antioxidant enzymes like TrxR can disrupt cellular ROS homeostasis, and defense against oxidative stress, thereby controlling a series of biological processes such as the cell proliferation, differentiation and death [18]. Cattaruzza et al. reported THA, gold(III)-dithiocarbamato derivatives which can strongly inhibit TrxR enzyme activity exhibit their anticancer activities in vitro and in vivo by stimulating the production of large amounts of ROS [59]. Chen et al. also found that the Ru(II) complex $[Ru(pip)_3]^{2+}$ which can inhibit TrxR activity displayed its antiproliferative activities against A375 cells by triggering intracellular ROS generation [14]. Thus, flow cytometry and inverted fluorescence microscope were used to detect the levels of intracellular ROS generation induced by Ru(II) complexes in A549 cells after staining with a DCFH-DA fluorescent dye. Figs. 5A and S21A showed that A549 cells treated with complexes **1** and **2** displayed obvious green fluorescence in comparison with DMSO-treated control, which suggests an increase in intracellular ROS level. The similar results are also observed by using flow cytometry. As seen in Figs. 5B and S21B, at a dose of 32 μM, treatment with complexes **1** or **2** for 6 h leads to significant rise in the mean fluorescent intensity (MFI) by rough 8.5-fold and 4.5-fold than control group, respectively. The data obtained from Figs. 5B and S21B suggest that complexes **1** and **2** significantly enhance cellular ROS level in a dose-dependent manner, and complex **1** induces more obvious ROS generation than complex **2**, which is positively correlated to their cytotoxicities and inhibitory activities of TrxR.

Besides, two ROS scavengers *N*-acetyl-L-cysteine (NAC) and glutathione (GSH) were used to explore the relationship between ROS and apoptosis. As shown in Fig. 5C, and D, both NAC and GSH notably inhibited the production of ROS and cell death induced by complex **1**. We further detected the percentage of apoptotic cells by Annexin V-FITC/PI staining assay after complex **1** treatment with or without antioxidants NAC or GSH. As shown in Fig. 5E, the percentage of apoptosis cells

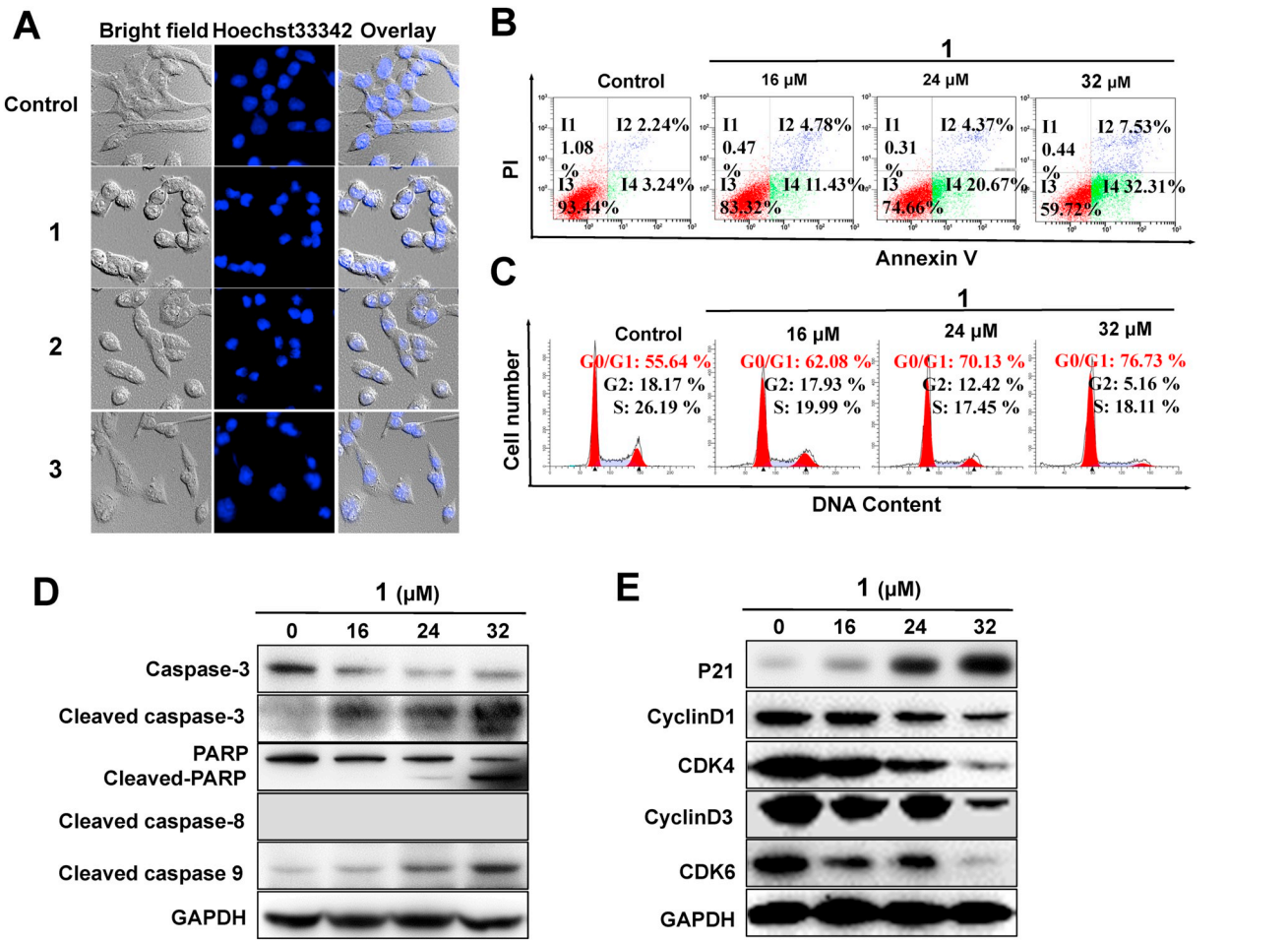

Fig. 4. (A) A549 cells stained with Hoechst 33342 after treatment of Ru(II) complexes at 32 μM for 24 h. (B) A549 cells apoptosis was detected by Annexin V/PI staining assay after co-incubation with various concentrations of complex **1** for 24 h. (C) Cell cycle distribution was performed by PI staining after co-incubated with complex **1** for 24 h.(D) The expression levels of caspase-3, PARP and cleaved caspase-3/8/9 and PARP were evaluated in a dose-dependent manner with complex **1** treatment for 24 h. (E) The effects of complex **1** on the expression levels of cell cycle relative proteins were performed by western blotting. GAPDH was used as internal control. A549 cells were treated with various concentrations of complex **1** for 24 h.

induced by complex **1** significantly reduced when ROS was inhibited by antioxidants. Taken together, the overproduction of ROS induced by complex **1** makes a great influence on inducing apoptosis in A549 cells.

3.7. Ru(II) complexes induce mitochondrial dysfunction

Since mitochondrion can release pro-apoptotic factors such as cytochrome *c* etc., it plays a critical role in apoptosis [60]. Mitochondrial dysfunction is involved in apoptotic process. Many anticancer Ru complexes can induce mitochondrial dysfunction by altering the MMP [12,13,30,31,44]. Therefore, we investigated the effects of Ru(II) complexes on the changes of MMP by using JC-1 as fluorescent probe. Mitochondrial depolarization is indicated by an increase in JC-1 green/red fluorescence intensity ratio. As indicated in Figs. 6A and S22A, the A549 cells displayed an obvious red-to-green color shift after incubation with complex **1** or complex **2**, displaying the loss of MMP in comparison with untreated cells. Next, we performed flow cytometry analysis to quantificationally detect the mitochondrial depolarization. As shown in Figs. 6B and S22B, there was a dose-dependent increase in the green fluorescence percentage. From Figs. 6B and S22B, complex **1** and complex **2** increased the JC-1 green fluorescence percentage from 2.45% (control) to 69.51% or 34.26% respectively, which demonstrating complex **1** caused more pronounced loss of MMP than complex **2**. These results indicate that both complex **1** and complex **2** can induce mitochondrial dysfunction contributing to cellular apoptosis in A549 cells.

Bcl-2 family members have been reported to play important roles in regulating mitochondrial function during Ru(II) complexes inducing cell apoptosis [31,61,62]. The decline of the Bcl-2 to Bax or Bcl-xl to Bad ratio could induce the permeabilization of mitochondria and lead to the release of cytochrome *c* into cytosol, which initiates the recruitment of caspase-9 and the formation of an apoptosome complex, causes caspase-3 activation and cell death [63–67]. Herein we investigated the mitochondrial pathway in apoptosis-induced by complex **1** through western blotting analysis. As presented in Fig. 6C, complex **1** treatment greatly up-regulated the level of proapoptotic proteins Bax and Bad, but down-regulated the level of prosurvival proteins Bcl-2 and Bcl-xl. The cytochrome *c* in cytosol was significantly increased. Combined with the results above, complex **1** triggers mitochondrial dysfunction and activates the mitochondria-mediated apoptotic pathway in A549 cells.

3.8. Complex 1 triggers DNA damage

A lot of Ru(II) complexes can trigger DNA damage, which is considered to be a hallmark of apoptosis [68–70]. Prior studies have confirmed that excess intracellular ROS can attack DNA, causing DNA damage and activating various damage sensor proteins such as ATM, Histone proteins, and the tumor suppressor gene p53 [71,72]. We have ascertained that complex **1** can induce ROS overproduction in A549

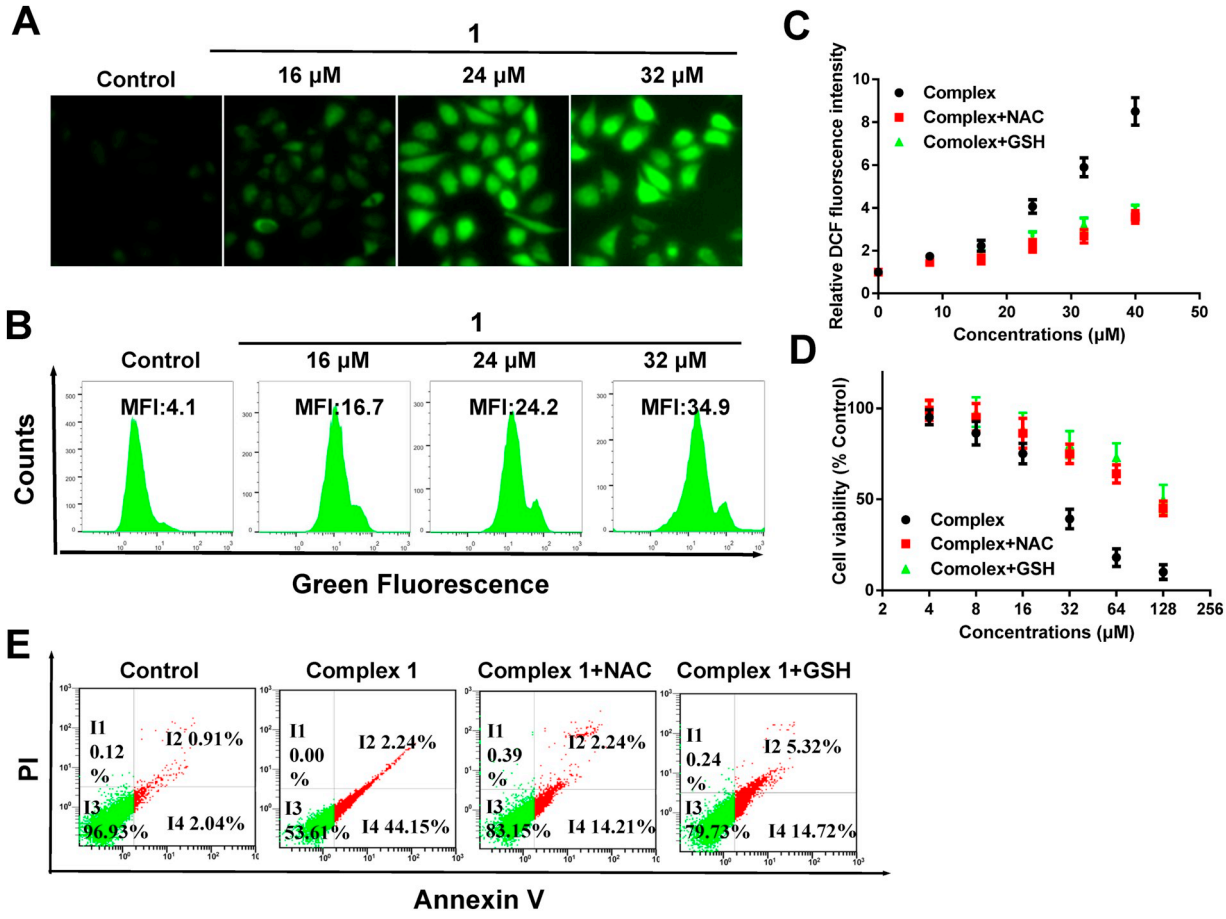

Fig. 5. (A) The cellular ROS level regulated by complex **1** was detected by inverted fluorescence microscope. (B) Flow cytometry analysis of cellular ROS level by DCFH-DA staining after different concentrations of complex **1** treatment for 12 h. (C) The suppression of GSH and NAC to ROS level regulated by complex **1**. (D) A549 cells were treated with different concentrations of complex **1** with or without antioxidants NAC (10 mM) or GSH (5 mM). Cell viability was assessed by MTT. (E) Cells apoptosis were detected by flow cytometry, A549 cells were treated with complex **1** for 24 h with or without pretreatment of NAC and GSH.

cells. Hence, single cell gel electrophoresis (comet assay) was performed to study whether, or not, complex **1** induced DNA damage. As expected, compared with untreated cells that fails to display a comet-like appearance, the cells incubated with complex **1** show well-formed comet tails (Fig. 7A), which indicates DNA damage has occurred. Western blotting was further performed to ascertain this. ATM and ATR, the central constituent of DNA damage response, control the initial phosphorylation of some pivotal proteins such as p53, checkpoint kinase 1/2 (Chk1 and Chk2) [73]. As illustrated in Fig. 7C, complex **1** up-regulated the phosphorylation levels of ATM, ATR, Chk1, Chk2, Histone and p53, which confirmed that complex **1** triggered DNA damage in A549 cells. However, when an antioxidant GSH was employed

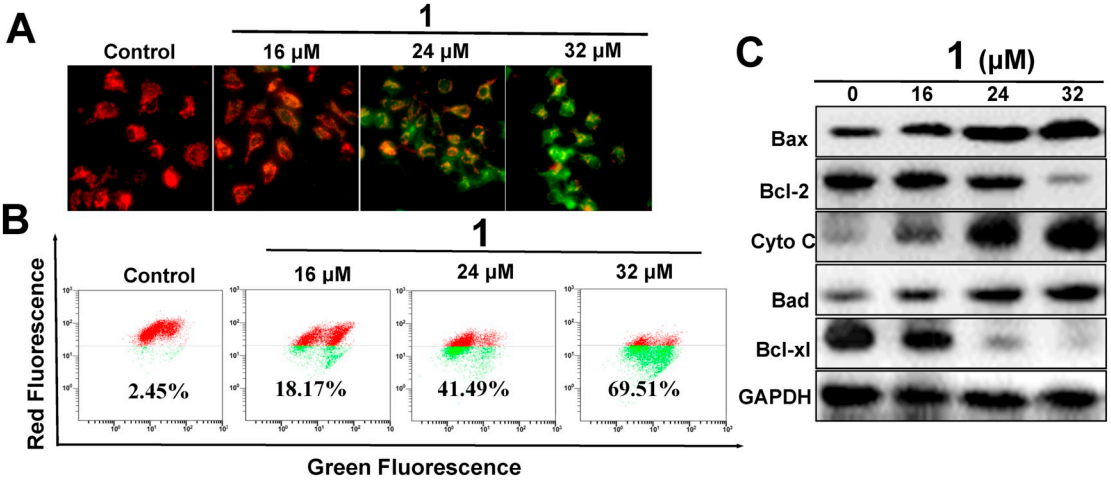

Fig. 6. Complex **1** induces mitochondrial dysfunction. (A) Fluorescence microscope analysis of cellular MMP level by JC-1 staining after different concentrations of complex **1** treatment for 24 h. (B) Flow cytometry analysis of cellular MMP level after different concentrations of complex **1** treatment for 24 h. (C) The influence exerted by complex **1** on the expression of Bcl-2 family proteins and cytochrome *c* in the cytosol.

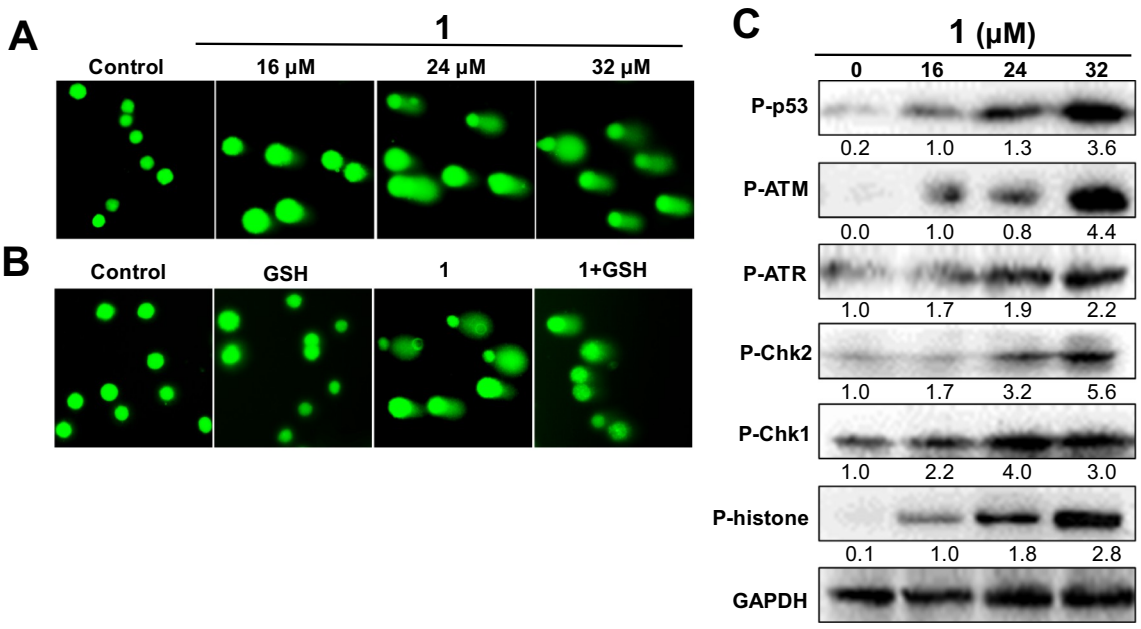

Fig. 7. (A) A549 cells were treated with various concentrations of complex **1** for 24 h, DNA fragmentation was examined by comet assay. (B) A549 cells were treated with 32 μM of complex **1** with or without antioxidants GSH (5 mM) for 24 h. (C) The expression levels of phosphorylated proteins ATM, ATR, Chk1, Chk2, Histone were performed by western blotting.

to pretreat the cells incubated with complex **1**, the lengths of comet tails were shortened (Fig. 7B). All these results suggest that complex **1** could trigger DNA fragmentation through excess intracellular ROS.

3.9. Complex 1 activates stress-response signaling pathways

MAPKs pathways, which consist of extracellular signal-regulated kinases (ERKs), Jun kinase (JNK) and p38, are primary oxidative stress-sensitive signal transduction pathways in most cell types [74]. Since complex **1** could induce the overproduction of superoxide in treated cancer cells, the expression of phosphorylation and total MAPKs were analyzed by western blotting. As seen in Fig. 8, the phosphorylation levels of JNK (p-JNK) and p38 (p-p38) were up-regulated in cells treated with complex **1**, while the phosphorylation of ERK (p-ERK) was down-regulated. AKT is also an crucial regulator in cellular processes, such as cell proliferation, survival and death, activation of which inhibits cell apoptosis and promotes cell proliferation [75]. Herein the results of western blotting analysis indicate that complex **1** suppresses the expression level of phosphorylation AKT (p-AKT) (Fig. 8). Altogether, these results demonstrate that synthetic Ru(II) complexes can inhibit TrxR and induce cell apoptosis through regulating MAPKs and AKT signaling.

4. Conclusions

In this study, three Ru(II) complexes of salicylate, [$Ru(phen)_2(SA)$] (**1**), [$Ru(dmb)_2(SA)$] (**2**) and [$Ru(bpy)_2(SA)$] (**3**), were synthesized, characterized and biologically evaluated. Complex **1** with highest lipophilicity exhibited highest absorption ratio and thus caused greatest anti-proliferation activities against A549 cells among three compounds. And complex **1** presented high selectivity between tumor cells and normal cell. Mechanism studies show that complex **1** can interact with TrxR and inhibit the activity of TrxR, which subsequently promotes the accumulation of ROS. Due to the overproduction of cellular ROS, oxidative stress-sensitive MAPKs signal pathway were activated, and the AKT signal pathway was suppressed, which leading to the acceleration of apoptosis process in A549 cells. Meanwhile, the overproduction of ROS initiated mitochondrial dysfunction, which regulated the

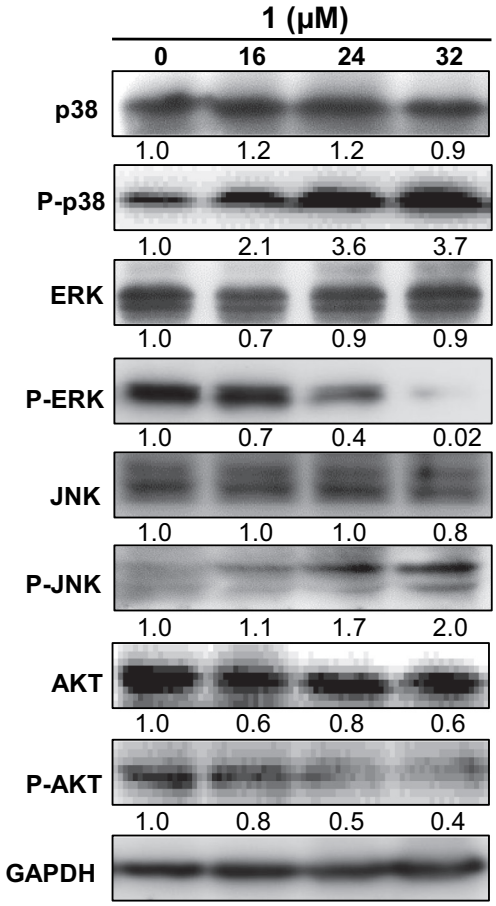

Fig. 8. A549 cells were incubated with different concentrations of complex **1** for 24 h. The effects of complex **1** on MAPKs and AKT signaling were assayed by western blotting assay.

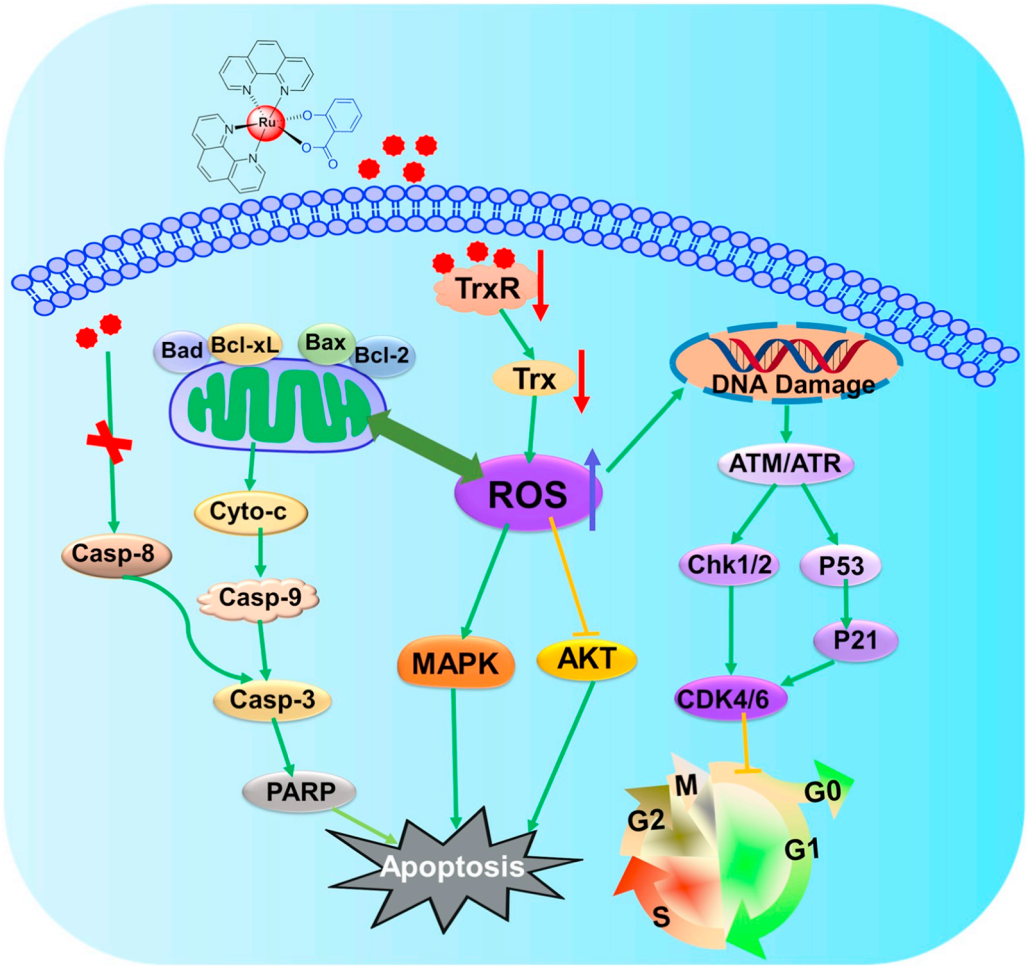

Fig. 9. Proposed signaling pathway triggered by complex **1** in A549 cells.

expression level of Bcl-2 family proteins, consequently, induced the release of apoptotic factors from mitochondrion and generated the cleavage of caspase family proteases. Additionally, it was found that complex **1** triggered notable DNA damage and caused cell cycle arrest in G0/G1 phase. In this study, the proposed apoptosis pathway generated by complex **1** in A549 cells is demonstrated in Fig. 9.

Altogether, the inhibition of TrxR by the synthetic Ru(II) complexes results in ROS-mediated apoptosis which involved of mitochondrial dysfunction, DNA damage, activation of MAPKs and inhibition of AKT signaling pathway. These results indicate that Ru(II) salicylate complexes may be developed as TrxR-targeted agents and potent anticancer drugs.

Abbreviations

A549	human lung carcinoma
HeLa	human cervical cancer
HepG2	human hepatocellular carcinoma
BEAS-2B	immortalized human bronchial epithelial cells
MCF-7	breast cancer
SA	salicylate
phen	1,10-phenanthroline
dmb	4,4′-dimethyl-2,2′-bipyridine
bpy	2,2′-bipyridine
pip	2-phenylimidazo[4,5-f] [1,10]phenanthroline
dppz	dipyrido[3,2-a:2′,3′-c]-phenazine
phpy	2-phenylpyridine
Sec	selenocysteine
Trx	thioredoxin
TrxR	thioredoxin reductase
GSH-Rs	glutathione reductase
GSH-Px	glutathione peroxidase
BSA	bovine serum albumin
MMP	mitochondrial membrane potential
BCA	bicinchoninic acid
DAPI	2-(4-amidinophenyl)-6-indolecarbamidine dihydrochloride
DCHF-DA	2′,7′-dichlorodihydrofluorescein diacetate
DMSO	dimethylsulfoxide
FBS	fetal bovine serum
JC-1	5,5′,6,6′-tetrachloro-1,1′,3,3′-tetrethylbenzimidalylcarbocyanine
MTT	3-(4,5-dimethylthiazole)-2,5-diphenyltetraazolium bromide
PBS	phosphate buffer saline
PI	propidium iodide
ROS	reactive oxygen species
GSH	glutathione
NAC	N-Acetyl-L-cysteine
RPMI	Roswell Park Memorial Institute
FITC	fluorescein isothiocyanate
ICP-MS	Inductively Coupled Plasma Mass Spectrometry
ESI-MS	Electrospary ionization mass spectrometry
PARP	poly(ADP-ribose) polymerase
CDK4	cyclin-dependent kinase 4
CDK6	cyclin-dependent kinase 6
Chk1	checkpoint kinase 1
Chk2	checkpoint kinase 2

MAPK mitogen activated protein kinase
AKT protein kinase B

Acknowledgements

This work was supported by the National Natural Science Foundation of China (No. 21701034), the Public Service Platform of South China Sea for R&D Marine Biomedicine Resources, Marine Biomedical Research Institute, Guangdong Medical University, the Medical Scientific Research Foundation of Guangdong Province of China (No. A2017309), the Natural Science Foundation of Guangdong Medical University (No. Z2017001), the Opening Project of Guangdong Province Key Laboratory of Computational Science at the Sun Yat-sen University (No. 2018017) and the University Student Innovation Experiment Program (No. 201810571039, 201810571067).

Appendix A. Supplementary data

Supplementary data to this article can be found online at https://doi.org/10.1016/j.jinorgbio.2019.01.011.

References

[1] S. Zha, V. Yegnasubramanian, W.G. Nelson, W.B. Isaacs, A.M. De Marzo, Cancer Lett. 215 (2004) 1–20.
[2] M. O'Connor, A. Kellett, M. McCann, G. Rosair, M. McNamara, O. Howe, B.S. Creaven, S. McClean, A. Foltyn-Arfa Kia, D. O'Shea, M. Devereux, J. Med. Chem. 55 (2012) 1957–1968.
[3] N. Palanisami, G. Prabusankar, R. Murugavel, Inorg. Chem. Commun. 9 (2006) 1002.
[4] M.A. Abdellah, S.K. Hadjikakou, N. Hadjiliadis, M. Kubicki, T. Bakas, N. Kourkoumelis, Y.V. Simos, S. Karkabounas, M.M. Barsan, I.S. Butler, Bioinorg. Chem. Appl. 2009 (2009) 12.
[5] C.N. Banti, A.D. Giannoulis, N. Kourkoumelis, A.M. Owczarzak, M. Kubicki, S.K. Hadjikakou, J. Inorg. Biochem. 142 (2015) 132–144.
[6] M. Poyraz, C.N. Banti, N. Kourkoumelis, V. Dokorou, M.J. Manos, M. Simčič, S. Golič-Grdadolnik, T. Mavromoustakos, A.D. Giannoulis, I.I. Verginadis, K. Charalabopoulos, S.K. Hadjikakou, Inorg. Chim. Acta 375 (2011) 114–121.
[7] C.N. Banti, A.D. Giannoulis, N. Kourkoumelis, A.M. Owczarzak, M. Poyraz, M. Kubicki, K. Charalabopoulos, S.K. Hadjikakou, Metallomics 4 (2012) 545–560.
[8] E.S. Antonarakis, A. Emadi, Cancer Chemother. Pharmacol. 66 (2010) 1–9.
[9] S. Leijen, S.A. Burgers, P. Baas, D. Pluim, M. Tibben, E. van Werkhoven, E. Alessio, G. Sava, J.H. Beijnen, J.H.M. Schellens, Investig. New Drugs 33 (2015) 201.
[10] S.W. Chang, A.R. Lewis, K.E. Prosser, J.R. Thompson, M. Gladkikh, M.B. Bally, J.J. Warren, C.J. Walsby, Inorg. Chem. 55 (2016) 4850.
[11] P. Heffeter, A. Riabtseva, Y. Senkiv, C.R. Kowol, W. Körner, U. Jungwith, N. Mitina, B.K. Keppler, T. Konstantinova, I. Yanchuk, R. Stoika, A. Zaichenko, W. Berger, J. Biomed. Nanotechnol. 10 (2014) 877.
[12] J. Chen, F. Peng, Y. Zhang, B. Li, J. She, X. Jie, Z. Zou, M. Chen, L. Chen, Eur. J. Med. Chem. 140 (2017) 104–117.
[13] L. Chen, G. Li, F. Peng, X. Jie, G. Dongye, K. Cai, R. Feng, B. Li, Q. Zeng, K. Lun, J. Chen, B. Xu, Oncotarget 7 (2016) 80716–80734.
[14] Z. Luo, L. Yu, F. Yang, Z. Zhao, B. Yu, H. Lai, K.-H. Wong, S.-M. Ngai, W. Zheng, T. Chen, Metallomics 6 (2014) 1480–1490.
[15] A. Meyer, C.P. Bagowski, M. Kokoschka, M. Stefanopoulou, H. Alborzinia, S. Can, D.H. Vlecken, W.S. Sheldrick, S. Wölfl, I. Ott, Angew. Chem. Int. Ed. 51 (2012) 8895–8899.
[16] L. He, S. Ji, H. Lai, T. Chen, J. Mater. Chem. B 3 (2015) 8383–8393.
[17] T.F. Whayne, N. Parinandi, N. Maulik, Can. J. Physiol. Pharmacol. 93 (2015) 903–911.
[18] E.S.J. Arnér, A. Holmgren, Semin. Cancer Biol. 16 (2006) 420–426.
[19] K.F. Tonissen, G.D. Trapani, Mol. Nutr. Food Res. 53 (2009) 87–103.
[20] E.S.J. Arnér, J. Nordberg, A. Holmgren, Biochem. Biophys. Res. Commun. 225 (1996) 268–274.
[21] N. Cenas, H. Nivinskas, Z. Anusevicius, J. Sarlauskas, F. Lederer, E.S. Arnér, J. Biol. Chem. 279 (2003) 2583–2592.
[22] L. Zhong, E.S.J. Arnér, A. Holmgren, Proc. Natl. Acad. Sci. 97 (2000) 5854–5859.
[23] V.N. Gladyshev, K.T. Jeang, T.C. Stadtman, Proc. Natl. Acad. Sci. 93 (1996) 6146–6151.
[24] F. Saccoccia, F. Angelucci, G. Boumis, D. Carotti, G. Desiato, A.E. Miele, A. Bellelli, Curr. Protein Pept. Sci. 15 (2014) 621–646.
[25] S. Prast-Nielsen, M. Cebula, I. Pader, E.S.J. Arnér, Free Radic. Biol. Med. 49 (2010) 1765–1778.
[26] W. Cai, L. Zhang, Y. Song, B. Wang, B. Zhang, X. Cui, G. Hu, Y. Liu, J. Wu, J. Fang, Free Radic. Biol. Med. 52 (2012) 257–265.
[27] R. Rubbiani, I. Kitanovic, H. Alborzinia, S. Can, A. Kitanovic, L.A. Onambele, M. Stefanopoulou, Y. Geldmacher, W.S. Sheldrick, G. Wolber, A. Prokop, S. Wölfl, I. Ott, J. Med. Chem. 53 (2010) 8608–8618.
[28] P. Mura, M. Camalli, A. Bindoli, F. Sorrentino, A. Casini, C. Gabbiani, M. Corsini, P. Zanello, M. Pia Rigobello, L. Messori, J. Med. Chem. 50 (2007) 5871–5874.
[29] A. Casini, C. Gabbiani, F. Sorrentino, M.P. Rigobello, A. Bindoli, T.J. Geldbach, A. Marrone, N. Re, C.G. Hartinger, P.J. Dyson, L. Messori, J. Med. Chem. 51 (2008) 6773–6781.
[30] L.M. Chen, F. Peng, G.D. Li, X.M. Jie, K.R. Cai, C. Cai, Y. Zhong, H. Zeng, W. Li, Z. Zhang, J.C. Chen, J. Inorg. Biochem. 156 (2016) 64.
[31] J. Chen, Y. Zhang, G. Li, F. Peng, X. Jie, J. She, G. Dongye, Z. Zou, S. Rong, L. Chen, J. Biol. Inorg. Chem. 23 (2018) 261–275.
[32] U. Schatzschneider, J. Niesel, I. Ott, R. Gust, H. Alborzinia, S. Wölfl, ChemMedChem 3 (2008) 1104–1109.
[33] C. Tan, S. Lai, S. Wu, S. Hu, L. Zhou, Y. Chen, M. Wang, Y. Zhu, W. Lian, W. Peng, L. Ji, A. Xu, J. Med. Chem. 53 (2010) 7613–7624.
[34] J.Q. Wang, P.Y. Zhang, C. Qian, X.J. Hou, L.N. Ji, H. Chao, J. Biol. Inorg. Chem. 19 (2014) 335–348.
[35] C. Tan, S. Wu, S. Lai, M. Wang, Y. Chen, L. Zhou, Y. Zhu, W. Lian, W. Peng, L. Ji, A. Xu, Dalton Trans. 40 (2011) 8611–8621.
[36] M.D. Hall, S. Amjadi, M. Zhang, P.J. Beale, T.W. Hambley, J. Inorg. Biochem. 98 (2004) 1614–1624.
[37] S.P. Oldfield, M.D. Hall, J.A. Platts, J. Med. Chem. 50 (2007) 5227–5237.
[38] S.H. van Rijt, A. Mukherjee, A.M. Pizarro, P.J. Sadler, J. Med. Chem. 53 (2010) 840–849.
[39] H. Huang, P. Zhang, H. Chen, L. Ji, H. Chao, Chem. Eur. J. 21 (2015) 715–725.
[40] A.J. Millett, A. Habtemariam, I. Romero-Canelón, G.J. Clarkson, P.J. Sadler, Organometallics 34 (2015) 2683–2694.
[41] S. Nikolić, L. Rangasamy, N. Gligorijević, S. Aranđelović, S. Radulović, G. Gasser, S. Grgurić-Šipka, J. Inorg. Biochem. 160 (2016) 156–165.
[42] S. Ulrich, N. Johanna, O. Ingo, G. Ronald, A. Hamed, W. Stefan, ChemMedChem 3 (2008) 1104–1109.
[43] R. Cao, J. Jia, X. Ma, M. Zhou, H. Fei, J. Med. Chem. 56 (2013) 3636–3644.
[44] H. Huang, P. Zhang, B. Yu, Y. Chen, J. Wang, L. Ji, H. Chao, J. Med. Chem. 57 (2014) 8971–8983.
[45] E.S.J. Arnér, Biochim. Biophys. Acta 1790 (2009) 495–526.
[46] S.K. Sandur, M.K. Pandey, B. Sung, K.S. Ahn, A. Murakami, G. Sethi, P. Limtrakul, V. Badmaev, B.B. Aggarwal, Carcinogenesis 28 (2007) 1765–1773.
[47] T. Zou, C.T. Lum, C.N. Lok, W.P. To, K.H. Low, C.M. Che, Angew. Chem. Int. Ed. 53 (2014) 5810–5814.
[48] L. Xie, Z. Luo, Z. Zhao, T. Chen, J. Med. Chem. 60 (2017) 202–214.
[49] W.-L. Kwong, C.-N. Lok, C.-W. Tse, E.L.-M. Wong, C.-M. Che, Chem. Eur. J. 21 (2015) 3062–3072.
[50] E.S.J. Arnér, H. Nakamura, T. Sasada, J. Yodoi, A. Holmgren, G. Spyrou, Free Radic. Biol. Med. 31 (2001) 1170–1178.
[51] K.K. Ooi, C.I. Yeo, T. Mahandaran, K.P. Ang, A.M. Akim, Y.-K. Cheah, H.-L. Seng, E.R.T. Tiekink, J. Inorg. Biochem. 166 (2017) 173–181.
[52] L. Cattaruzza, D. Fregona, M. Mongiat, L. Ronconi, A. Fassina, A. Colombatti, D. Aldinucci, Int. J. Cancer 128 (2011) 206–215.
[53] P.R. Florindo, D.M. Pereira, P.M. Borralho, C.M.P. Rodrigues, M.F.M. Piedade, A.C. Fernandes, J. Med. Chem. 58 (2015) 4339–4347.
[54] P. Wu, S.Y. Liu, J.Y. Su, J.P. Chen, L. Li, R.G. Zhang, T.F. Chen, Food Funct. 8 (2017) 3707.
[55] H. Lai, Z. Zhao, L. Li, W. Zheng, T. Chen, Metallomics 7 (2015) 439–447.
[56] C. Wang, Z. Li, M. Fu, T. Bouras, R.G. Pestell, Signal transduction mediated by cyclin D1: from mitogens to cell proliferation: a molecular target with therapeutic potential, in: R. Kumar (Ed.), Molecular Targeting and Signal Transduction, Springer, 2004, pp. 217–237.
[57] T. Abbas, A. Dutta, Nat. Rev. Cancer 9 (2009) 400.
[58] L.-W.W. Su-Hua Huang, An-Cheng Huang, Chien-Chih Yu, Jin-Cherng Lien, Yi-Ping Huang, Jai-Sing Yang, Jen-Hung Yang, Yu-Ping Hsiao, W. Gibson Wood, Chun-Shu Yu, Jing-Gung Chung, J. Agric. Food Chem. 60 (2012) 665–675.
[59] L. Cattaruzza, D. Fregona, M. Mongiat, L. Ronconi, A. Fassina, A. Colombatti, D. Aldinucci, Int. J. Cancer 128 (2011) 206–215.
[60] K. Wang, X. Fu, X. Fu, Y. Hou, J. Fang, S. Zhang, M. Yang, D. Li, L. Mao, J. Sun, H. Yuan, X. Yang, C. Fan, Z. Zhang, B. Sun, Mol. Neurobiol. 53 (2016) 4363–4374.
[61] L. Li, Y.-S. Wong, T. Chen, C. Fan, W. Zheng, Dalton Trans. 41 (2012) 1138–1141.
[62] C. Qian, J.Q. Wang, C. Song, L.L. Wang, L.N. Ji, H. Chao, Metallomics 5 (2013) 844–854.
[63] S. Willis, C.L. Day, M.G. Hinds, D.C.S. Huang, J. Cell Sci. 116 (2003) 4053–4056.
[64] J. Zhou, S. Zhang, O. Choon-Nam, H.-M. Shen, Biochem. Pharmacol. 72 (2006) 132–144.
[65] D.R. Green, J.C. Reed, Science 281 (1998) 1309–1312.
[66] H. Zhou, A. Aguilar, J. Chen, L. Bai, L. Liu, J.L. Meagher, C.-Y. Yang, D. McEachern, X. Cong, J.A. Stuckey, S. Wang, J. Med. Chem. 55 (2012) 6149–6161.
[67] A.K. Larsen, A. Escargueil, A. Skladanowski, Prog. Cell Cycle Res. 5 (2003) 295–300.
[68] W.P. Roos, B. Kaina, Trends Mol. Med. 12 (2006) 440–450.
[69] L.F. Magalhães, F. Mello-Andrade, W.C. Pires, H.D. Silva, P.F.F. da Silva, L.M. Macedo, C. Henrique de Castro, C.C. Carneiro, C.G. Cardoso, P.R. de Melo Reis, L. Camargo de Oliveira, R.R. Caetano, A.A. Batista, E.d.P. Silveira-Lacerda, Chem. Biol. Interact. 278 (2017) 101–113.
[70] S. Swavey, K. Morford, M. Tsao, K. Comfort, M.K. Kilroy, J. Inorg. Biochem. 175 (2017) 101–109.
[71] S.W. Lee, M.H. Lee, J.H. Park, S.H. Kang, H.M. Yoo, S.H. Ka, Y.M. Oh, Y.J. Jeon, C.H. Chung, EMBO J. 31 (2012) 4441–4452.
[72] C. Fan, J. Chen, Y. Wang, Y.-S. Wong, Y. Zhang, W. Zheng, W. Cao, T. Chen, Free Radic. Biol. Med. 65 (2013) 305–316.
[73] B.-B.S. Zhou, S.J. Elledge, Nature 408 (2000) 433–439.
[74] T. Boutros, E. Chevet, P. Metrakos, Pharmacol. Rev. 60 (2008) 261–310.
[75] K.R. Park, D. Nam, H.M. Yun, S.G. Lee, H.J. Jang, G. Sethi, S.K. Cho, K.S. Ahn, Cancer Lett. 312 (2011) 178.